This is the accepted manuscript made available via CHORUS. The article has been published as:

First observation of the isospin violating decay J/ψ→ΛΣ[over ¯]^{0}+c.c.

M. Ablikim *et al.* (BESIII Collaboration)

Phys. Rev. D **86**, 032008 — Published 15 August 2012

DOI: 10.1103/PhysRevD.86.032008

First observation of the isospin violating decay $J/\psi \to \Lambda\bar{\Sigma}^0 + c.c.$

M. Ablikim[1], M. N. Achasov[5], D. J. Ambrose[39], F. F. An[1], Q. An[40], Z. H. An[1], J. Z. Bai[1], Y. Ban[27], J. Becker[2], N. Berger[1], M. Bertani[18A], J. M. Bian[38], E. Boger[20,a], O. Bondarenko[21], I. Boyko[20], R. A. Briere[3], V. Bytev[20], X. Cai[1], O. Cakir[35A], A. Calcaterra[18A], G. F. Cao[1], S. A. Cetin[35B], J. F. Chang[1], G. Chelkov[20,a], G. Chen[1], H. S. Chen[1], J. C. Chen[1], M. L. Chen[1], S. J. Chen[25], Y. Chen[1], Y. B. Chen[1], H. P. Cheng[14], Y. P. Chu[1], D. Cronin-Hennessy[38], H. L. Dai[1], J. P. Dai[1], D. Dedovich[20], Z. Y. Deng[1], A. Denig[19], I. Denysenko[20,b], M. Destefanis[43A,43C], W. M. Ding[29], Y. Ding[23], L. Y. Dong[1], M. Y. Dong[1], S. X. Du[46], J. Fang[1], S. S. Fang[1], L. Fava[43B,43C], F. Feldbauer[2], C. Q. Feng[40], R. B. Ferroli[18A], C. D. Fu[1], J. L. Fu[25], Y. Gao[34], C. Geng[40], K. Goetzen[7], W. X. Gong[1], W. Gradl[19], M. Greco[43A,43C], M. H. Gu[1], Y. T. Gu[9], Y. H. Guan[6], A. Q. Guo[26], L. B. Guo[24], Y.P. Guo[26], Y. L. Han[1], X. Q. Hao[1], F. A. Harris[37], K. L. He[1], M. He[1], Z. Y. He[26], T. Held[2], Y. K. Heng[1], Z. L. Hou[1], H. M. Hu[1], J. F. Hu[6], T. Hu[1], B. Huang[1], G. M. Huang[15], J. S. Huang[12], X. T. Huang[29], Y. P. Huang[1], T. Hussain[42], C. S. Ji[40], Q. Ji[1], X. B. Ji[1], X. L. Ji[1], L. K. Jia[1], L. L. Jiang[1], X. S. Jiang[1], J. B. Jiao[29], Z. Jiao[14], D. P. Jin[1], S. Jin[1], F. F. Jing[34], N. Kalantar-Nayestanaki[21], M. Kavatsyuk[21], W. Kuehn[36], W. Lai[1], J. S. Lange[36], C. H. Li[1], Cheng Li[40], Cui Li[40], D. M. Li[46], F. Li[1], G. Li[1], H. B. Li[1], J. C. Li[1], K. Li[10], Lei Li[1], N. B. Li[24], Q. J. Li[1], S. L. Li[1], W. D. Li[1], W. G. Li[1], X. L. Li[29], X. N. Li[1], X. Q. Li[26], X. R. Li[28], Z. B. Li[33], H. Liang[40], Y. F. Liang[31], Y. T. Liang[36], G. R. Liao[34], X. T. Liao[1], B. J. Liu[1], C. L. Liu[3], C. X. Liu[1], C. Y. Liu[1], F. H. Liu[30], Fang Liu[1], Feng Liu[15], H. Liu[1], H. B. Liu[6], H. H. Liu[13], H. M. Liu[1], H. W. Liu[1], J. P. Liu[44], K. Y. Liu[23], Kai Liu[6], Kun Liu[27], P. L. Liu[29], S. B. Liu[40], X. Liu[22], X. H. Liu[1], Y. Liu[1], Y. B. Liu[26], Z. A. Liu[1], Zhiqiang Liu[1], Zhiqing Liu[1], H. Loehner[21], G. R. Lu[12], H. J. Lu[14], J. G. Lu[1], Q. W. Lu[30], X. R. Lu[6], Y. P. Lu[1], C. L. Luo[24], M. X. Luo[45], T. Luo[37], X. L. Luo[1], M. Lv[1], C. L. Ma[6], F. C. Ma[23], H. L. Ma[1], Q. M. Ma[1], S. Ma[1], T. Ma[1], X. Y. Ma[1], Y. Ma[11], F. E. Maas[11], M. Maggiora[43A,43C], Q. A. Malik[42], H. Mao[1], Y. J. Mao[27], Z. P. Mao[1], J. G. Messchendorp[21], J. Min[1], T. J. Min[1], R. E. Mitchell[17], X. H. Mo[1], C. Morales Morales[11], C. Motzko[2], N. Yu. Muchnoi[5], H. Muramatsu[39], Y. Nefedov[20], C. Nicholson[6], I. B. Nikolaev[5], Z. Ning[1], S. L. Olsen[28], Q. Ouyang[1], S. Pacetti[18B], J. W. Park[28], M. Pelizaeus[37], H. P. Peng[40], K. Peters[7], J. L. Ping[24], R. G. Ping[1], R. Poling[38], E. Prencipe[19], M. Qi[25], S. Qian[1], C. F. Qiao[6], X. S. Qin[1], Y. Qin[27], Z. H. Qin[1], J. F. Qiu[1], K. H. Rashid[42], G. Rong[1], X. D. Ruan[9], A. Sarantsev[20,c], B. D. Schaefer[17], J. Schulze[2], M. Shao[40], C. P. Shen[37,d], X. Y. Shen[1], H. Y. Sheng[1], M. R. Shepherd[17], X. Y. Song[1], S. Spataro[43A,43C], B. Spruck[36], D. H. Sun[1], G. X. Sun[1], J. F. Sun[12], S. S. Sun[1], X. D. Sun[1], Y. J. Sun[40], Y. Z. Sun[1], Z. J. Sun[1], Z. T. Sun[40], C. J. Tang[31], X. Tang[1], X. F. Tang[8] I. Tapan[35C], E. H. Thorndike[39], H. L. Tian[1], D. Toth[38], M. Ullrich[36], G. S. Varner[37], B. Wang[9], B. Q. Wang[27], K. Wang[1], L. L. Wang[4], L. S. Wang[1], M. Wang[29], P. Wang[1], P. L. Wang[1], Q. Wang[1], Q. J. Wang[1], S. G. Wang[27], X. L. Wang[40], Y. D. Wang[40], Y. F. Wang[1], Y. Q. Wang[29], Z. Wang[1], Z. G. Wang[1], Z. Y. Wang[1], D. H. Wei[8], P. Weidenkaff[19], Q. G. Wen[40], S. P. Wen[1], M. Werner[36], U. Wiedner[2], L. H. Wu[1], N. Wu[1], S. X. Wu[40], W. Wu[26], Z. Wu[1], L. G. Xia[34], Z. J. Xiao[24], Y. G. Xie[1], Q. L. Xiu[1], G. F. Xu[1], G. M. Xu[27], H. Xu[1], Q. J. Xu[10], X. P. Xu[32], Z. R. Xu[40], F. Xue[15], Z. Xue[1], L. Yan[40], W. B. Yan[40], Y. H. Yan[16], H. X. Yang[1], Y. Yang[15], Y. X. Yang[8], H. Ye[1], M. Ye[1], M. H. Ye[4], B. X. Yu[1], C. X. Yu[26], J. S. Yu[22], S. P. Yu[29], C. Z. Yuan[1], W. L. Yuan[24], Y. Yuan[1], A. A. Zafar[42], A. Zallo[18A], Y. Zeng[16], B. X. Zhang[1], B. Y. Zhang[1], C. C. Zhang[1], D. H. Zhang[1], H. H. Zhang[33], H. Y. Zhang[1], J. Zhang[24], J. Q. Zhang[1], J. W. Zhang[1], J. Y. Zhang[1], J. Z. Zhang[1], S. H. Zhang[1], T. R. Zhang[24], X. J. Zhang[1], X. Y. Zhang[29], Y. Zhang[1], Y. H. Zhang[1], Y. S. Zhang[9], Z. P. Zhang[40], Z. Y. Zhang[44], G. Zhao[1], H. S. Zhao[1], J. W. Zhao[1], K. X. Zhao[24], Lei Zhao[40], Ling Zhao[1], M. G. Zhao[26], Q. Zhao[1], S. J. Zhao[46], T. C. Zhao[1], X. H. Zhao[25], Y. B. Zhao[1], Z. G. Zhao[40], A. Zhemchugov[20,a], B. Zheng[41], J. P. Zheng[1], Y. H. Zheng[6], Z. P. Zheng[1], B. Zhong[1], J. Zhong[2], L. Zhou[1], X. K. Zhou[6], X. R. Zhou[40], C. Zhu[1], K. Zhu[1], K. J. Zhu[1], S. H. Zhu[1], X. L. Zhu[34], X. W. Zhu[1], Y. C. Zhu[40], Y. M. Zhu[26], Y. S. Zhu[1], Z. A. Zhu[1], J. Zhuang[1], B. S. Zou[1], J. H. Zou[1], J. X. Zuo[1]

(BESIII Collaboration)

[1] *Institute of High Energy Physics, Beijing 100049, P. R. China*
[2] *Bochum Ruhr-University, 44780 Bochum, Germany*
[3] *Carnegie Mellon University, Pittsburgh, PA 15213, USA*
[4] *China Center of Advanced Science and Technology, Beijing 100190, P. R. China*
[5] *G.I. Budker Institute of Nuclear Physics SB RAS (BINP), Novosibirsk 630090, Russia*
[6] *Graduate University of Chinese Academy of Sciences, Beijing 100049, P. R. China*
[7] *GSI Helmholtzcentre for Heavy Ion Research GmbH, D-64291 Darmstadt, Germany*
[8] *Guangxi Normal University, Guilin 541004, P. R. China*
[9] *GuangXi University, Nanning 530004,P.R.China*
[10] *Hangzhou Normal University, Hangzhou 310036, P. R. China*
[11] *Helmholtz Institute Mainz, J.J. Becherweg 45,D 55099 Mainz,Germany*
[12] *Henan Normal University, Xinxiang 453007, P. R. China*
[13] *Henan University of Science and Technology, Luoyang 471003, P. R. China*
[14] *Huangshan College, Huangshan 245000, P. R. China*
[15] *Huazhong Normal University, Wuhan 430079, P. R. China*
[16] *Hunan University, Changsha 410082, P. R. China*
[17] *Indiana University, Bloomington, Indiana 47405, USA*
[18] *(A)INFN Laboratori Nazionali di Frascati, Frascati, Italy; (B)INFN and University of Perugia, I-06100, Perugia, Italy*
[19] *Johannes Gutenberg University of Mainz, Johann-Joachim-Becher-Weg 45, 55099 Mainz, Germany*
[20] *Joint Institute for Nuclear Research, 141980 Dubna, Russia*
[21] *KVI/University of Groningen, 9747 AA Groningen, The Netherlands*

[22] Lanzhou University, Lanzhou 730000, P. R. China
[23] Liaoning University, Shenyang 110036, P. R. China
[24] Nanjing Normal University, Nanjing 210046, P. R. China
[25] Nanjing University, Nanjing 210093, P. R. China
[26] Nankai University, Tianjin 300071, P. R. China
[27] Peking University, Beijing 100871, P. R. China
[28] Seoul National University, Seoul, 151-747 Korea
[29] Shandong University, Jinan 250100, P. R. China
[30] Shanxi University, Taiyuan 030006, P. R. China
[31] Sichuan University, Chengdu 610064, P. R. China
[32] Soochow University, Suzhou 215006, China
[33] Sun Yat-Sen University, Guangzhou 510275, P. R. China
[34] Tsinghua University, Beijing 100084, P. R. China
[35] (A)Ankara University, Ankara, Turkey; (B)Dogus University, Istanbul, TURKEY; (C)Uludag University, Bursa, Turkey
[36] Universitaet Giessen, 35392 Giessen, Germany
[37] University of Hawaii, Honolulu, Hawaii 96822, USA
[38] University of Minnesota, Minneapolis, MN 55455, USA
[39] University of Rochester, Rochester, New York 14627, USA
[40] University of Science and Technology of China, Hefei 230026, P. R. China
[41] University of South China, Hengyang 421001, P. R. China
[42] University of the Punjab, Lahore-54590, Pakistan
[43] (A)University of Turin, Turin, Italy; (B)University of Eastern Piedmont, Alessandria, Italy; (C)INFN, Turin, Italy
[44] Wuhan University, Wuhan 430072, P. R. China
[45] Zhejiang University, Hangzhou 310027, P. R. China
[46] Zhengzhou University, Zhengzhou 450001, P. R. China

[a] also at the Moscow Institute of Physics and Technology, Moscow, Russia
[b] on leave from the Bogolyubov Institute for Theoretical Physics, Kiev, Ukraine
[c] also at the PNPI, Gatchina, Russia
[d] now at Nagoya University, Nagoya, Japan

Using a sample of $(225.2 \pm 2.8) \times 10^6$ J/ψ events collected with the BESIII detector, we present results of a study of $J/\psi \to \gamma\Lambda\bar{\Lambda}$ and report the first observation of the isospin violating decay $J/\psi \to \Lambda\bar{\Sigma}^0 + c.c.$, in which $\bar{\Sigma}^0$ decays to $\gamma\bar{\Lambda}$. The measured branching fractions are $\mathcal{B}(J/\psi \to \bar{\Lambda}\Sigma^0)$ $= (1.46 \pm 0.11 \pm 0.12) \times 10^{-5}$ and $\mathcal{B}(J/\psi \to \Lambda\bar{\Sigma}^0) = (1.37 \pm 0.12 \pm 0.11) \times 10^{-5}$. We search for $\Lambda(1520) \to \gamma\Lambda$ decay, and find no evident signal, and an upper limit for the product branching fraction $\mathcal{B}(J/\psi \to \Lambda\bar{\Lambda}(1520) + c.c.) \times \mathcal{B}(\Lambda(1520) \to \gamma\Lambda) < 4.1 \times 10^{-6}$ is set at the 90% confidence level. We also report the observation of $\eta_c \to \Lambda\bar{\Lambda}$ in $J/\psi \to \gamma\eta_c$, $\eta_c \to \Lambda\bar{\Lambda}$ and measure the branching fraction $\mathcal{B}(\eta_c \to \Lambda\bar{\Lambda}) = (1.16 \pm 0.12(\text{stat}) \pm 0.19(\text{syst}) \pm 0.28(\text{PDG})) \times 10^{-3}$.

PACS numbers: 13.25.Gv, 12.38.Qk, 13.60.Rj, 14.20.Jn

I. INTRODUCTION

The study of charmonium meson decays into baryon pairs is an important field that intersects particle and nuclear physics, and provides novel means for exploring various properties of baryons [1]. The decay $J/\psi \to \bar{\Lambda}\Sigma^0 + c.c.$ is an isospin symmetry breaking decay, and a measurement of its branching fraction will help elucidate isospin-breaking mechanisms in $J/\psi \to B_8\bar{B}_8$ decays [2, 3]. Until now, only an upper limit on the branching fraction of $\mathcal{B}(J/\psi \to \bar{\Lambda}\Sigma^0 + c.c.) < 1.5 \times 10^{-4}$ has been set at the 90% confidence level (C.L.) by the Mark I Collaboration, based on a study of $J/\psi \to \gamma\Lambda\bar{\Lambda}$ [4].

The electromagnetic decays of hyperons $\Lambda^* \to \gamma\Lambda$ provide clean probes for examining the internal structure of Λ^* hyperon resonances [5]. For example, predictions for the radiative decay $\Lambda(1520) \to \gamma\Lambda$ have been made in a number of frameworks including: a non-relativistic quark model (NRQM) [6, 7]; a relativistic constituent quark model (RCQM) [8]; the MIT bag model [6]; the chiral bag model [9]; an algebraic model of hadron structure [10]; and a chiral quark model (χQM) [11]. In contrast, experimental measurements have been sparse [12–15]. The radiative decays $\Lambda^* \to \gamma\Lambda$ can be studied with $J/\psi \to \gamma\Lambda\bar{\Lambda}$ events.

The $J/\psi \to \gamma\Lambda\bar{\Lambda}$ events can also originate from radiative $J/\psi \to \gamma\eta_c$ decays followed by η_c decays to $\Lambda\bar{\Lambda}$. To date, $\eta_c \to \Lambda\bar{\Lambda}$ has only been observed in $B^\pm \to \Lambda\bar{\Lambda}K^\pm$ decays by the Belle experiment [16]. A measurement of $\eta_c \to \Lambda\bar{\Lambda}$ in J/ψ radiative decays provides useful information in addition to Belle's measurement in B decays.

In this paper, we report the first observation of the isospin violating decay $J/\psi \to \Lambda\bar{\Sigma}^0 + c.c.$, a new measurement of the branching fraction for $\eta_c \to \Lambda\bar{\Lambda}$ and the results of a search for the radiative decay $\Lambda(1520) \to \gamma\Lambda$.

II. DETECTOR AND MONTE CARLO SIMULATIONS

The analysis is based on analyses of $J/\psi \to \gamma\Lambda\bar{\Lambda}$ events contained in a sample of $(225.2 \pm 2.8) \times 10^6$ J/ψ events [17] accumulated with the Beijing Spectrometer III (BESIII) operating at the Beijing Electron-Position Collider II (BEPCII) [18].

BEPCII is a double ring e^+e^- collider with a design peak luminosity of $10^{33}\mathrm{cm}^{-2}\mathrm{s}^{-1}$ with beam currents of 0.93 A. The BESIII detector consists of a cylindrical core comprised of a helium-based main drift chamber (MDC), a plastic scintillator time-of-flight (TOF) system, and a CsI(Tl) electromagnetic calorimeter (EMC) that are all enclosed in a superconducting solenoidal magnet that provides a 1.0 T axial magnetic field. The solenoid is supported by an octagonal flux-return yoke that contains resistive-plate-chamber muon-identifier modules interleaved with plates of steel. The acceptance for charged particles and photons is 93% of 4π sr, and the charged-particle momentum and photon energy resolutions at 1 GeV are 0.5% and 2.5%, respectively.

The responses of the BESIII detector are modeled with a Monte Carlo (MC) simulation based on GEANT4 [19, 20]. EVTGEN [21] is used to generate $J/\psi \to \Lambda\bar{\Sigma}^0 + c.c.$ events with an angular distribution of $1 + \alpha\cos^2\theta$, where θ is the polar angle of the baryon in the J/ψ rest frame and α is a parameter extracted in fits to data described below. The $J/\psi \to \gamma\eta_c$ decays are generated with an angular distribution of $1 + \cos^2\theta_\gamma$ and a phase space distribution for $\eta_c \to \Lambda\bar{\Lambda}$, and effect of spin-correlation is not considered in the MC simulation for $\eta_c \to \Lambda\bar{\Lambda}$ decay. Inclusive J/ψ decays are produced by the MC event generator KKMC [22], the known J/ψ decay modes are generated by EVTGEN [21] with branching fractions set at their Particle Data Group (PDG) world average values [23], and the remaining unknown decays are generated with LUNDCHARM [24].

III. DATA ANALYSIS

Charged tracks in the BESIII detector are reconstructed from track-induced signals in the MDC. We select tracks within ± 20 cm of the interaction point in the beam direction and within 10 cm in the plane perpendicular to the beam; the track directions are required to be within the MDC fiducial volume, $|\cos\theta| < 0.93$. Candidate events are required to have four charged tracks with net charge zero. The $\Lambda\bar{\Lambda}$ pair is reconstructed using the $\Lambda \to p\pi^-$, and $\bar{\Lambda} \to \bar{p}\pi^+$ decay modes. We loop over all the combinations of positive and negative charged track pairs and require that at least one $(p\pi^-)(\bar{p}\pi^+)$ track hypothesis successfully passes the Λ and $\bar{\Lambda}$'s vertex finding algorithm.

If there is more than one accepted $(p\pi^-)(\bar{p}\pi^+)$ combination in an event, the candidate with minimum value of $(M_{p\pi^-} - M_\Lambda)^2 + (M_{\bar{p}\pi^+} - M_{\bar{\Lambda}})^2$ is selected, where $M_{p\pi^-}$ ($M_{\bar{p}\pi^+}$) and M_Λ ($M_{\bar{\Lambda}}$) are the measured mass and its expected value. Since there are differences in the detection efficiencies between data and the MC simulation for low-momentum proton and antiprotons [25], we reject events containing any proton or antiproton track candidate with momentum below 0.3 GeV/c.

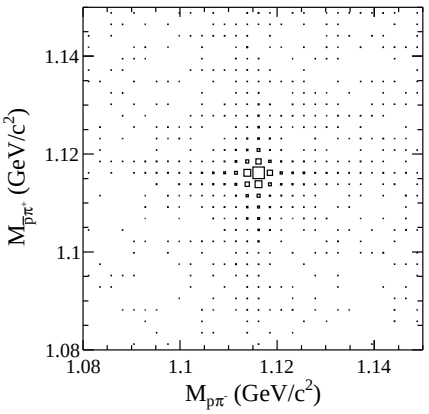

FIG. 1: A scatter plot of $M_{p\pi^-}$ *versus* $M_{\bar{p}\pi^+}$ for selected candidate events.

Electromagnetic showers are reconstructed from clusters of energy deposits in the EMC. The energy deposited in nearby TOF counters is added to improve the reconstruction efficiency and energy resolution. Showers identified as photon candidates are required to satisfy fiducial and shower-quality requirements: *e.g.*, showers in the barrel region ($|\cos\theta| < 0.80$) must have a minimum energy of 25 MeV, while those from end caps ($0.86 < |\cos\theta| < 0.92$) must have at least 50 MeV. To suppress showers generated by charged particles, we require that the photon candidate direction is at least 5° away from its nearest proton and charged pion tracks, and at least 30° away from the nearest antiproton track, since more EMC showers tend to be found near the direction of the antiproton. This requirement decreases the signal efficiency by 18% for $J/\psi \to \Lambda\bar{\Sigma}^0(\bar{\Sigma}^0 \to \gamma\bar{\Lambda})$ compared to that for $J/\psi \to \bar{\Lambda}\Sigma^0(\Sigma^0 \to \gamma\Lambda)$ since the photon from the radiative $\bar{\Sigma}^0 \to \gamma\bar{\Lambda}$ decay is closer to the direction of the antiproton. Requirements on the EMC cluster timing are used to suppress electronic noise and energy deposits that are unrelated to the event. A four-constraint (4C) energy-momentum conservation kinematic fit is performed to the $\gamma\Lambda\bar{\Lambda}$ hypothesis. For events with more than one photon candidate, the combination with the minimum χ^2_{4C} is selected. In addition, we also require $\chi^2_{4C} < 45$ in order to suppress backgrounds from the decays $J/\psi \to \Lambda\bar{\Lambda}$, $\Sigma^0\bar{\Sigma}^0$ and $\Lambda\bar{\Lambda}\pi^0$.

A scatter plot of $M_{p\pi^-}$ *versus* $M_{\bar{p}\pi^+}$ for events that survive the above requirements is shown in Fig. 1), where a cluster of Λ and $\bar{\Lambda}$ signals is evident. To select $J/\psi \to \gamma\Lambda\bar{\Lambda}$ signal events, we require $|M_{p\pi^-} - M_\Lambda| < 5$ MeV/c^2 and $|M_{\bar{p}\pi^+} - M_{\bar{\Lambda}}| < 5$ MeV/c^2. An $M^2(\gamma\bar{\Lambda})$ (vertical) *versus* $M^2(\gamma\Lambda)$ (horizontal) Dalitz plot for these events

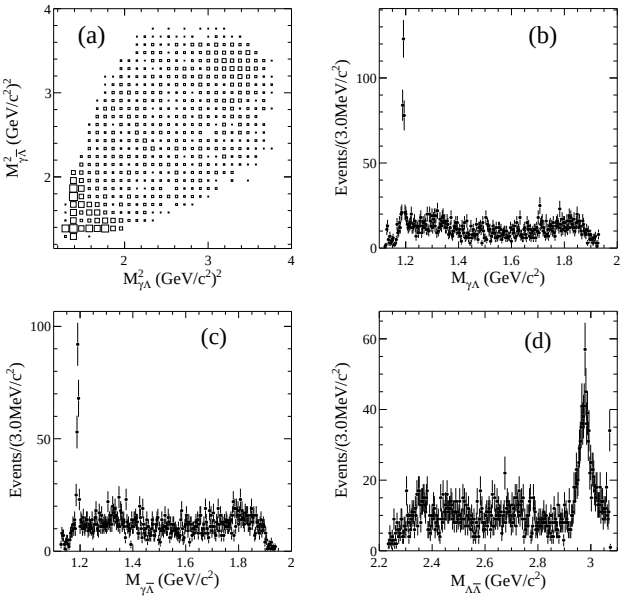

FIG. 2: (a) An $M^2(\gamma\bar{\Lambda})$ (vertical) *versus* $M^2(\gamma\Lambda)$ (horizontal) Dalitz plot for selected events and the (b) $\gamma\Lambda$, (c) $\gamma\bar{\Lambda}$ & (d) $\Lambda\bar{\Lambda}$ invariant mass distributions for the selected $J/\psi \to \gamma\Lambda\bar{\Lambda}$ event sample.

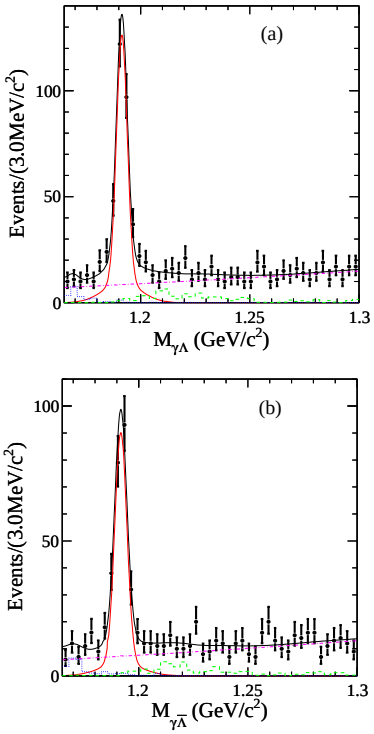

FIG. 3: The results of the fit for the Σ^0 (a) and $\bar{\Sigma}^0$ (b). The points with error bars are data. The fit results are shown by the black solid curves. The light (red) solid curves are the signal shapes. The (blue) dotted-histograms are from the normalized $J/\psi \to \Lambda\bar{\Lambda}$ background; the (green) dashed-histograms are from the normalized $J\psi \to \Sigma^0\bar{\Sigma}^0$ background. The (magenta) dot-dashed curves show the non-resonant (phase space) background polynomial.

is shown in Fig. 2 (a); the $\gamma\Lambda$ and $\gamma\bar{\Lambda}$ mass spectra are shown in Fig. 2 (b) and (c). Prominent signals of the Σ^0 and $\bar{\Sigma}^0$, corresponding to $J/\psi \to \Lambda\bar{\Sigma}^0 + c.c.$ decays, are observed. On the other hand, no obvious signal for $\Lambda(1520) \to \gamma\Lambda$ is seen. A clear η_c signal can be seen in the $\Lambda\bar{\Lambda}$ mass spectrum shown in Fig. 2 (d), while no significant enhancement at other $\Lambda\bar{\Lambda}$ masses is evident.

For the $J/\psi \to \Lambda\bar{\Sigma}^0 + c.c.$ study, we apply the same requirements to a sample of 225 million MC-simulated inclusive J/ψ events and find that the primary backgrounds come from $J/\psi \to \Lambda\bar{\Lambda}$, $\Sigma^0\bar{\Sigma}^0$ and $\Lambda\bar{\Lambda}\pi^0$ decays, where either a cluster in the EMC unrelated to the event is misidentified as a photon candidate or one of the the photons from the $\Sigma^0\bar{\Sigma}^0$ or π^0 decay is undetected in the EMC. Normalized $M(\gamma\Lambda)$ and $M(\gamma\bar{\Lambda})$ distributions from the events that survive the application of the 4C kinematic fit, shown as dotted- and dashed-histograms in Figs. 3 (a) and (b), show no sign of peaking in the Σ^0 or $\bar{\Sigma}^0$ mass regions. Another potential source of background is from $J/\psi \to \gamma\eta_c$ ($\eta_c \to \Lambda\bar{\Lambda}$) decay and non-resonant $J/\psi \to \gamma\Lambda\bar{\Lambda}$, which contribute a smooth background under the signal region, shown as dot-dashed curves in Figs. 3 (a) and (b). The expected backgrounds are 105 ± 10 (95 ± 9) events in the Σ^0 ($\bar{\Sigma}^0$) signal region for $J/\psi \to \bar{\Lambda}\Sigma^0$ ($J/\psi \to \Lambda\bar{\Sigma}^0$) as listed in Table I. The signal region is defined as being within $\pm 3\sigma$ of the nominal Σ^0 ($\bar{\Sigma}^0$) mass. It should be noted that the background events from the non-resonant $J/\psi \to \gamma\Lambda\bar{\Lambda}$ are not counted and are accounted for by the floating polynomial function discussed below.

Unbinned maximum likelihood (ML) fits are used to determine the $\Lambda\bar{\Sigma}^0$ and $\bar{\Lambda}\Sigma^0$ event yields. The signal probability density function (PDF) for Σ^0 ($\bar{\Sigma}^0$) from $J/\psi \to \bar{\Lambda}\Sigma$ ($\Lambda\bar{\Sigma}^0$) is represented by a double Gaussian function with parameters determined from the MC simulation except for the Gaussian widths, which are allowed to float. Backgrounds from $J/\psi \to \Lambda\bar{\Lambda}$ and $\Sigma^0\bar{\Sigma}^0$ are fixed to their MC simulations at their expected intensities. The remaining background is described by a second-order polynomial function with parameters that are allowed to float. The fitting ranges for both the Σ^0 and the $\bar{\Sigma}^0$ are $1.165 - 1.30$ GeV/c^2. Figures 3 (a) and (b) show the results of the fits to Σ^0 and $\bar{\Sigma}^0$. The fitted yields are 308 ± 24 and 234 ± 21 signal events for $J/\psi \to \bar{\Lambda}\Sigma^0$ and $\Lambda\bar{\Sigma}^0$, respectively. The goodness of fit is estimated by using a χ^2 test method with the data distributions regrouped to ensure that each bin contains more than 10 events. The test gives $\chi^2/n.d.f = 28.1/37 = 0.76$ for $J/\psi \to \bar{\Lambda}\Sigma^0$ and $\chi^2/n.d.f = 43.5/37 = 1.2$ for $J/\psi \to \Lambda\bar{\Sigma}^0$.

In the higher $\gamma\Lambda$ ($\gamma\bar{\Lambda}$) invariant mass regions, shown in Figs. 2 (b) and (c), no obvious signals for $\Lambda(1520) \to \gamma\Lambda$ ($\bar{\Lambda}(1520) \to \gamma\bar{\Lambda}$) are evident. We require that the invariant mass of $\Lambda\bar{\Lambda}$ is less than 2.9 GeV/c^2 to further suppress combinatorial backgrounds from $J/\psi \to \Lambda\bar{\Lambda}$,

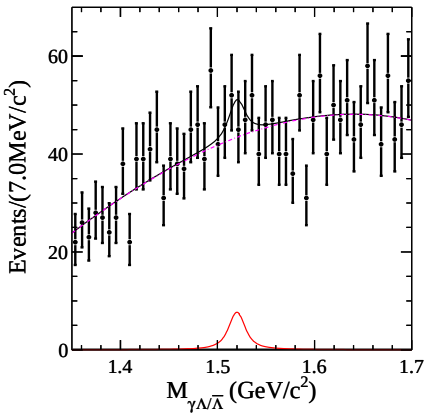

FIG. 4: The results of the fit for the $\Lambda(1520)$. The points with error bars are data. The fit result is shown by the black solid curve; the (magenta) dashed curve is the background polynomial and the (red) light solid curve is the $\Lambda(1520)$ signal shape. (Here the $M(\gamma\Lambda)$ and $M(\gamma\bar{\Lambda})$ mass distributions are combined.)

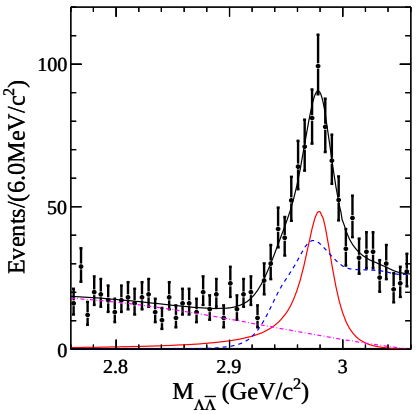

FIG. 5: The η_c mass distribution and fit results. Points with error bars are data. The fit result is shown as a black solid curve, the (red) light solid curve is the signal shape, the (blue) dashed curve is the combined incoherent background from the $J/\psi \to \Sigma^0\bar{\Sigma}^0$, $\Lambda\bar{\Sigma}^0 + c.c.$, the (magenta) dot-dashed-curve is the non-resonant background.

$\Sigma^0\bar{\Sigma}^0$, $\Lambda\bar{\Lambda}\pi^0$ and $J/\psi \to \gamma\eta_c(\eta_c \to \Lambda\bar{\Lambda})$ decays. After the above requirement, only 14 ± 1 events from these background decay modes remain. In the surviving combined $M(\gamma\Lambda)$ and $M(\gamma\bar{\Lambda})$ mass spectrum, shown in Fig. 4, there is no evidence for a $\Lambda(1520)$ signal above expectations for a phase space distribution of $J/\psi \to \gamma\Lambda\bar{\Lambda}$.

In the ML fit to the Fig. 4 distribution, the $\Lambda(1520)$ signal PDF is represented by a Breit-Wigner (BW) function convolved with a double-Gaussian resolution function, with parameters determined from the fit to the Σ^0 data. The shape for the non-resonant background is described by a second-order polynomial function, and the background yield and its PDF parameters are allowed to float in the fit. The mass range used for the $\Lambda(1520)$ fit is $1.35 - 1.70$ GeV/c^2. Figure 4 shows the result of the fit to $\Lambda(1520)$, which returns a $\Lambda(1520)$ signal yield of 31 ± 24 events. The goodness of the fit is $\chi^2/n.d.f = 45.9/45 = 1.02$. Using a Bayesian method, an upper limit for the number of $\Lambda(1520)$ signal events is determined to be 62.5 at the 90% confidence level (C.L.). The signal yields and the efficiencies for the analyses of $J/\psi \to \bar{\Lambda}\Sigma^0$ ($\Lambda\bar{\Sigma}^0$) and $\Lambda\bar{\Lambda}(1520) + c.c.$ are summarized in Table I.

For the $J/\psi \to \gamma\eta_c(\eta_c \to \Lambda\bar{\Lambda})$ analysis, the dominant backgrounds remaining after event selection are from $J/\psi \to \Sigma^0\bar{\Sigma}^0$ and $\Lambda\bar{\Sigma}^0 + c.c.$. The expected number of events in the signal region from these two sources is 637 ± 52, as listed in Table I. These backgrounds are incoherent (*i.e.,* do not interfere with the η_c signal amplitude). In addition, there is an irreducible background from non-resonant $J/\psi \to \gamma\Lambda\bar{\Lambda}$ decays that is potentially coherent with the signal process (*i.e.,* may interfere with the η_c signal amplitude).

For the η_c fit, the combined incoherent background is fixed to the shape and level of the MC simulation. The PDF for the coherent non-resonant background is

TABLE I: For each decay mode, the number of signal events (N_S), the number of expected background events (N_B) in the signal region (non-resonant $J/\psi \to \gamma\Lambda\bar{\Lambda}$ background is excluded), and the MC efficiency (ε) for signal are given. The error on N_S is statistical only, and the signal regions are defined to be within $\pm 3\sigma$ of the nominal Σ^0 and $\Lambda(1520)$ masses.

Modes	N_S	N_B	$\epsilon(\%)$
$J/\psi \to \bar{\Lambda}\Sigma^0(\Sigma^0 \to \gamma\Lambda)$	308 ± 24	105 ± 10	21.7
$J/\psi \to \Lambda\bar{\Sigma}^0(\bar{\Sigma}^0 \to \gamma\bar{\Lambda})$	234 ± 21	95 ± 9	17.6
$J/\psi \to \Lambda\bar{\Lambda}(1520) + c.c.(\bar{\Lambda}(1520) \to \gamma\bar{\Lambda})$	31 ± 24	14 ± 1	18.8
$J/\psi \to \gamma\eta_c(\eta_c \to \Lambda\bar{\Lambda})$	360 ± 38	637 ± 52	19.8

described by a second-order polynomial, with yield and shape parameters that are floated in the fit. For the lineshape for η_c mesons produced via the M1 transition, we use $(E_\gamma^3 \times \mathrm{BW}(m) \times \mathrm{damping}(E_\gamma)) \otimes \mathrm{Gauss}(0,\sigma)$, where m is the $\Lambda\bar{\Lambda}$ invariant mass, $E_\gamma = \frac{M_{J/\psi}^2 - m^2}{2M_{J/\psi}}$ is the energy of the transition photon in the rest frame of J/ψ, damping(E_γ) is a function that damps the divergent low-mass tail produced by the E_γ^3 factor, and Gauss$(0,\sigma)$ is a Gaussian function that describes the detector resolution. The damping function used by the KEDR [26] collaboration for a related process has the form:

$$\frac{E_0^2}{E_0 E_\gamma + (E_0 - E_\gamma)^2}, \qquad (1)$$

where $E_0 = \frac{M_{J/\psi}^2 - M_{\eta_c}^2}{2M_{J/\psi}}$ is the peak energy of the transition photon. On the other hand, the CLEO experiment damped the E_γ^3 term by a factor $\exp(-E_\gamma^2/8\beta^2)$, with $\beta = 65$ MeV [27], to account for the difference in overlap of the ground state wave functions. We use the KEDR function in our default fit and use the CLEO function

as an alternative. The difference between the results obtained with the two damping functions is considered as a systematic error associated with uncertainties in the line shape. In the fit, the mass and width of η_c are fixed to the recent BESIII measurements: $M(\eta_c) = 2984.3 \pm 0.8$ MeV/c^2 and $\Gamma(\eta_c) = 32.0 \pm 1.6$ MeV [28], and interference between the non-resonant background and the η_c resonance amplitude is neglected [30]. The mass range used for the η_c fit is $2.76-3.06$ GeV/c^2. Figure 5 shows the result of the fit to η_c, which yields (360 ± 38) signal events. The goodness of the fit is $\chi^2/n.d.f = 42.7/43 = 0.99$. The signal yield and efficiency are summarized in Table I.

IV. SYSTEMATIC UNCERTAINTIES

The systematic uncertainties on the branching fraction measurements are summarized in Table II. The systematic uncertainty due to the charged tracking efficiency has been studied with control samples of $J/\psi \to pK^-\bar{\Lambda} + c.c.$ and $J/\psi \to \Lambda\bar{\Lambda}$ decays. The difference in the charged tracking efficiency between data and the MC simulation is 1% per track. The uncertainty due to the Λ and $\bar{\Lambda}$ vertex fit is determined to be 1% for each Λ by using the same control samples. The uncertainty due to the photon reconstruction is determined to be 1% for each photon [17]. The uncertainties due to the kinematic fit are determined by comparing the efficiency as a function of χ^2_{4C} value for the MC samples and the control samples of $J/\psi \to \Lambda\bar{\Lambda}$ and $J/\psi \to \Sigma^0\bar{\Sigma}^0$ events, in which zero and two photons are involved in the final states. The differences in the efficiencies between data and MC simulation are 2.1% and 2.3% from the studies of $J/\psi \to \Lambda\bar{\Lambda}$ and $J/\psi \to \Sigma^0\bar{\Sigma}^0$ events, respectively; we use 2.3% as the systematic error due to the kinematic fit.

The signal shape for the Σ^0 ($\bar{\Sigma}^0$) is described by a double-Gaussian function and the widths are floated in the nominal fit. An alternative fit is performed by fixing the signal shape to the MC simulation, and the systematic uncertainty is set based on the change observed in the yield. In the fit to $\Lambda(1520)$, since the shape of the signal is obtained from MC simulation, the uncertainty is estimated by changing the mass and width of $\Lambda(1520)$ by one standard deviation from their PDG world average values [23]. This systematic error is determined in this way to be 4.8%.

In the η_c fit, the mass resolution is fixed to the MC simulation; the level of possible discrepancy is determined with a smearing Gaussian, for which a non-zero σ would represent a MC-data difference in the mass resolution. The uncertainty associated with a difference determined in this way is 1.1%. Changes in the mass and width of the η_c used in the fit by one standard deviation from the recently measured BESIII values [28], produce a relative change in the signal yield of 6.4%. As mentioned above, damping functions from the KEDR and CLEO collaborations were used in the fit to suppress the lower mass tail produced by the E_γ^3 factor; the relative difference in the yields between the two fits is 3.9%. The 7.6% quadrature sum of these uncertainties is used as the systematical error associated with uncertainties in η_c signal line-shape.

For the measurement of the $J/\psi \to \bar{\Lambda}\Sigma^0$ ($\Lambda\bar{\Sigma}^0$), the expected number of background events from the decays of $J/\psi \to \Lambda\bar{\Lambda}$ and $\Sigma^0\bar{\Sigma}^0$ is fixed in the fit. To estimate the associated uncertainty, we vary the number of expected background events by one standard deviation from the PDG branching fraction values [23], which gives an uncertainty of 0.6% (0.4%) for the $J/\psi \to \bar{\Lambda}\Sigma^0$ ($\Lambda\bar{\Sigma}^0$). In the ML fit to η_c, the incoherent backgrounds from $J/\psi \to \Sigma^0\bar{\Sigma}^0$ and $\bar{\Lambda}\Sigma^0 + c.c.$ are also fixed at their expected numbers of events. The uncertainty associated with this is determined by changing the number of expected incoherent background events by one standard deviation of the PDG branching fraction values [23] for the $J/\psi \to \Sigma^0\bar{\Sigma}^0$ and the measured value for $J/\psi \to \bar{\Lambda}\Sigma^0 + c.c.$ from the analysis reported here; the resulting change in the η_c signal yield is 12.8%.

The uncertainty due to the non-resonant background shape for each mode has been estimated by changing the polynomial order from two to three. The systematic uncertainties due to the fitting ranges are evaluated by changing them from $1.165-1.30$ GeV/c^2 to $1.165-1.25$ GeV/c^2 (Σ^0 and $\bar{\Sigma}^0$), from $1.35-1.70$ GeV/c^2 to $1.38-1.67$ GeV/c^2 ($\Lambda(1520)$) and from $2.76-3.06$ GeV/c^2 to $2.70-3.06$ GeV/c^2 (η_c). The changes in yields for these variations give systematic uncertainties due to the choices of fitting ranges, as shown in Table II.

The electromagnetic cross sections for $\Lambda\bar{\Sigma}^0 + c.c.$ production through direct one-photon exchange and J/ψ decay in e^+e^- can be inferred using the factorization hypothesis to be [29]:

$$\frac{\sigma(e^+e^- \to \gamma^* \to \Lambda\bar{\Sigma}^0)}{\sigma(e^+e^- \to J/\psi \to \Lambda\bar{\Sigma}^0)} \approx \frac{\sigma(e^+e^- \to \gamma^* \to \mu^+\mu^-)}{\sigma(e^+e^- \to J/\psi \to \mu^+\mu^-)}. \quad (2)$$

Neglecting interference between $e^+e^- \to \gamma^* \to \mu^+\mu^-$ and $e^+e^- \to J/\psi \to \mu^+\mu^-$, one can obtain, at $\sqrt{s} = 3.097$ GeV, $\sigma(e^+e^- \to J/\psi \to \mu^+\mu^-) = \mathcal{B}(J/\psi \to \mu^+\mu^-) \times \frac{N_{J/\psi}}{\mathcal{L}} = 168 \pm 3.2$ nb, where $N_{J/\psi}$ and $\mathcal{L}$ are the number of total J/ψ events ($225.2 \pm 2.8 \times 10^6$) and the corresponding integrated luminosity (79631 ± 70(stat.) $\pm$ 796(syst.)) nb [17], respectively. At $\sqrt{s} = 3.097$ GeV, $\sigma_{\rm Born}(e^+e^- \to \gamma^* \to \mu^+\mu^-)$ is 9.05 nb. From this we estimate the relative ratio of the QED background from $e^+e^- \to \gamma^* \to \Lambda\bar{\Sigma}^0 + c.c.$ to be (5.4 ± 0.1)% of our measured yield of $J/\psi \to \Lambda\bar{\Sigma}^0 + c.c.$ events. Therefore, we adjust our result be a factor of 0.946 when we determine the $J/\psi \to \bar{\Lambda}\Sigma^0 + c.c.$ branching fraction value; we use 0.1% as a systematic error due to the uncertainty in this correction factor.

The angular distribution of the baryon in $J/\psi \to B_8\bar{B}_8$ decay is expected to have a $1 + \alpha\cos^2\theta$ behaviour. Figures 6 (a) and (b) show the distributions of $\cos\theta$ for $\bar{\Lambda}$ ($J/\psi \to \bar{\Lambda}\Sigma^0$) and Λ ($J/\psi \to \Lambda\bar{\Sigma}^0$), respectively, after correcting the signal yields for the detection efficiency. A simultaneous fit to the angular distributions

TABLE II: Summary of systematic errors for the branching fraction measurements (%).

	$J/\psi \to \bar{\Lambda}\bar{\Sigma}^0$	$J/\psi \to \Lambda\bar{\Sigma}^0$	$J/\psi \to \Lambda\bar{\Lambda}(1520) + c.c. \to \gamma\Lambda\bar{\Lambda}$	$J/\psi \to \gamma\eta_c \to \gamma\Lambda\bar{\Lambda}$
Photon detection	1	1	1	1
Tracking	4	4	4	4
Λ and $\bar{\Lambda}$ vertex fits	2	2	2	2
4C kinematic fit	2.3	2.3	2.3	2.3
Signal shape	1.3	2.6	4.8	7.6
Fitting range	1.6	0.9	1.4	1.4
α	5.5	5.1	10.2	-
Fixed backgrounds	0.6	0.4	-	12.8
Non-resonant background shape	0.3	0.1	1.9	1.7
QED correction factor	0.1	0.1	-	-
Cited branching fractions	0.8	0.8	0.8	0.8
Number of J/ψ	1.3	1.3	1.3	1.3
Total systematic uncertainty	8.0	7.9	12.6	16.0

for $\bar{\Lambda}$ and Λ returns the value $\alpha = 0.38 \pm 0.39$. The detection efficiencies are determined with MC simulation for $J/\psi \to \Lambda\bar{\Sigma}^0 + c.c.$ using $\alpha = 0.38$ in the signal MC generator. To estimate the uncertainty originating from the parameter α, we generate MC samples for $\alpha = 0.38$ and for other values in the range $0.0 \sim 0.77$. The maximum difference is 5.1% (5.5%) for $J/\psi \to \Lambda\bar{\Sigma}^0$ ($\bar{\Lambda}\Sigma^0$) and is taken as a systematic error. For $J/\psi \to \Lambda\bar{\Lambda}(1520)+c.c.$ decay, the detection efficiency is obtained with a phase-space MC simulation. We generate MC samples for $\alpha = 0$ and $\alpha = 1$ to estimate the uncertainty due to the unknown parameter α. The difference of efficiency of 10.2% is taken as systematic error for the $J/\psi \to \Lambda\bar{\Lambda}(1520) + c.c.$.

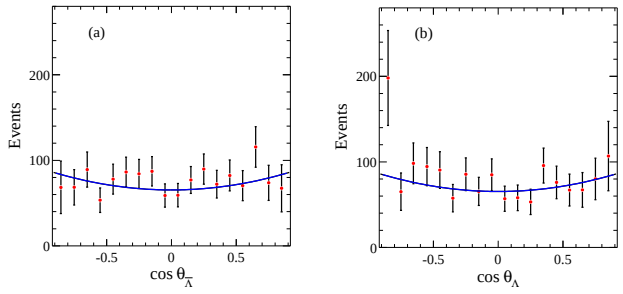

FIG. 6: The corrected distributions of $\cos\theta$ for $\bar{\Lambda}$ from $J/\psi \to \bar{\Lambda}\bar{\Sigma}^0$ decay (a), for Λ from $J/\psi \to \Lambda\bar{\Sigma}^0$ decay (b). The curves in (a) and (b) present the fits to the function $1+\alpha\cos^2\theta$. The goodness of the fits are $\chi^2/n.d.f = 21/18 = 1.2$ for $\bar{\Lambda}$ and $\chi^2/n.d.f = 29/18 = 1.6$ for Λ.

The branching fraction for the $\Lambda \to p\pi$ decay is taken from the PDG [23]; the 0.8% uncertainty is taken as a systematic uncertainty in our measurements. The uncertainty in the number of J/ψ decays in our data sample is 1.3% [17]. The total systematic uncertainties for the branching fraction measurements are obtained by adding up the contributions from all the systematic sources in quadrature as summarized in Table II.

V. RESULTS AND DISCUSSION

The branching fractions are calculated with $\mathcal{B} = N_S/(N_{J/\psi}\epsilon\mathcal{B}^2_{p\pi})$, where N_S and ϵ are the number of signal events and the detection efficiency, listed in Table I. Here $N_{J/\psi} = (225.2\pm2.8)\times10^6$ [17] is the number of J/ψ events, and $\mathcal{B}_{p\pi}$ is the branching fraction of the $\Lambda \to p\pi$ taken from the PDG [23]. The calculated branching fractions, along with the PDG [23] limits, are listed in Table III.

TABLE III: Branching fractions (10^{-5}) from this analysis, where the first errors are statistical and the second ones are systematic, and the PDG values [23] for comparison. The upper limits are at the 90% C.L..

J/ψ decay mode	BESIII	PDG
$\bar{\Lambda}\bar{\Sigma}^0$	$1.46 \pm 0.11 \pm 0.12$	< 7.5
$\Lambda\bar{\Sigma}^0$	$1.37 \pm 0.12 \pm 0.11$	< 7.5
$\gamma\eta_c(\eta_c \to \Lambda\bar{\Lambda})$	$1.98 \pm 0.21 \pm 0.32$	-
$\Lambda\bar{\Lambda}(1520) + c.c.(\bar{\Lambda}(1520) \to \gamma\bar{\Lambda})$	< 0.41	-

Our measurement of the branching fraction for $J/\psi \to \Lambda\bar{\Sigma}^0 + c.c.$ decay can shed light on the $SU(3)$ breaking mechanism. The amplitude for J/ψ decay to a pair of octet baryons can be parameterized in terms of a $SU(3)$ singlet A, as well as symmetric and antisymmetric charge-breaking (D, F) and mass-breaking (D', F') terms, as described in Refs. [2, 3, 31] and listed in Table IV, where δ is used to designate the relative phase between the one-photon and gluon-mediated hadronic decay amplitudes. According to this amplitude parameterizations the $J/\psi \to \bar{\Lambda}\bar{\Sigma}^0 + c.c.$ branching fraction mea-

TABLE IV: Amplitude parameterizations from [2, 3, 31] for J/ψ decay to a pair of octet baryons. General expressions in terms of a singlet A, as well as symmetric and antisymmetric charge-breaking (D, F) and mass-breaking terms ($D^{'}$, $F^{'}$) are given. Here δ is the relative phase between one-photon and gluon mediated hadronic decay amplitudes. Except for the branching fraction for $J/\psi \to \Lambda\bar{\Sigma}^0 + c.c.$ decay (marked with an asterisk) from this measurement and for $J/\psi \to p\bar{p}$, $n\bar{n}$ from the recent BESIII measurements [32], the other branching fractions ($\mathcal{B}$) are taken from the PDG [23].

Decay mode	Amplitude	$\mathcal{B}(\times 10^{-3})$
$p\bar{p}$	$A + e^{i\delta}(D+F) + D^{'} + F^{'}$	(2.112 ± 0.031) [32]
$n\bar{n}$	$A - e^{i\delta}(2D) + D^{'} + F^{'}$	(2.07 ± 0.17) [32]
$\Sigma^+\bar{\Sigma}^-$	$A + e^{i\delta}(D+F) - 2D^{'}$	(1.50 ± 0.24)
$\Sigma^0\bar{\Sigma}^0$	$A + e^{i\delta}(D) - 2D^{'}$	(1.29 ± 0.09)
$\Xi^0\bar{\Xi}^0$	$A - e^{i\delta}(2D) + D^{'} - F^{'}$	(1.20 ± 0.24)
$\Xi^-\bar{\Xi}^+$	$A + e^{i\delta}(D-F) + D^{'} - F^{'}$	(0.85 ± 0.16)
$\Lambda\bar{\Lambda}$	$A - e^{i\delta}(D) + 2D^{'}$	(1.61 ± 0.15)
$\bar{\Lambda}\Sigma^0(\Lambda\bar{\Sigma}^0)$	$(\sqrt{3}D)$	$(0.014 \pm 0.002)^*$

surement is important for the determination of the symmetric charge-breaking term D. In Ref. [31], a constrained fit to the measured branching fractions of $J/\psi \to B_8\bar{B}_8$ is performed to extract the values of the parameters A, F, D', F' and δ using the Table IV amplitude parameterizations. In the previous fit [31], $D = 0$ was assumed, *i.e.,* $\mathcal{B}(J/\psi \to \Lambda\bar{\Sigma}^0 + c.c.) = 0$. We perform another fit that includes our new measurement and includes a nonzero value for D. The fit results are listed in Table V. In comparison to the Ref. [31] results, the value for the relative phase δ has changed significantly, while the A, D', F and F' values do not change significantly. The measurement of the isospin-violating decay $J/\psi \to \bar{\Lambda}\Sigma^0 + c.c.$ also provides useful information on the mechanisms for $J/\psi \to B_8\bar{B}_{10}$ decays, where the large A-term is absent [2, 3].

VI. SUMMARY

In summary, with a sample of $(225.2 \pm 2.8) \times 10^6$ J/ψ events in the BESIII detector, the $J/\psi \to \gamma\Lambda\bar{\Lambda}$ decay has been studied. The branching fractions of $J/\psi \to \bar{\Lambda}\Sigma^0$, $J/\psi \to \Lambda\bar{\Sigma}^0$ and $J/\psi \to \gamma\eta_c(\eta_c \to \Lambda\bar{\Lambda})$ are measured for the first time as: $\mathcal{B}(J/\psi \to \bar{\Lambda}\Sigma^0) = (1.46 \pm 0.11 \pm 0.12) \times 10^{-5}$, $\mathcal{B}(J/\psi \to \Lambda\bar{\Sigma}^0) = (1.37 \pm 0.12 \pm 0.11) \times 10^{-5}$ and $\mathcal{B}(J/\psi \to \gamma\eta_c) \times \mathcal{B}(\eta_c \to \Lambda\bar{\Lambda}) = (1.98 \pm 0.21 \pm 0.32) \times 10^{-5}$, respectively, where the uncertainties are statistical and systematic. Using the PDG value [23] for $J/\psi \to \gamma\eta_c$, we obtain $\mathcal{B}(\eta_c \to \Lambda\bar{\Lambda}) = (1.16 \pm 0.12 \pm 0.19 \pm 0.28\ (\mathrm{PDG})) \times 10^{-3}$, where the third error is from the error on $\mathcal{B}(J/\psi \to \gamma\eta_c)$. Using $B^{\pm} \to \Lambda\bar{\Lambda}K^{\pm}$ decay the Belle experiment measured $\mathcal{B}(\eta_c \to \Lambda\bar{\Lambda}) = (0.87^{+0.24+0.09}_{-0.21-0.14} \pm 0.27\ (\mathrm{PDG})) \times 10^{-3}$ [16], which is consistent with our result within error. No evidence for the decay of $J/\psi \to \Lambda\bar{\Lambda}(1520) + c.c.$ is found, and an upper limit for the branching fraction is determined to be $\mathcal{B}(J/\psi \to \Lambda\bar{\Lambda}(1520) + c.c.) \times \mathcal{B}(\Lambda(1520) \to \gamma\Lambda) < 4.1 \times 10^{-6}$ at the 90% confidence level. Results are listed in Table III and compared with previous measurements.

Acknowledgments

The BESIII collaboration thanks the staff of BEPCII and the computing center for their hard efforts. This work is supported in part by the Ministry of Science and Technology of China under Contract No. 2009CB825200; National Natural Science Foundation of China (NSFC) under Contracts Nos. 10625524, 10821063, 10825524, 10835001, 10935007, 11125525; Joint Funds of the National Natural Science Foundation of China under Contracts Nos. 11079008, 11179007; the Chinese Academy of Sciences (CAS) Large-Scale Scientific Facility Program; CAS under Contracts Nos. KJCX2-YW-N29, KJCX2-YW-N45; 100 Talents Program of CAS; Istituto Nazionale di Fisica Nucleare, Italy; Ministry of Development of Turkey under Contract No. DPT2006K-120470; U. S. Department of Energy under Contracts Nos. DE-FG02-04ER41291, DE-FG02-91ER40682, DE-FG02-94ER40823; U.S. National Science Foundation; University of Groningen (RuG) and the Helmholtzzentrum fuer Schwerionenforschung GmbH (GSI), Darmstadt; WCU Program of National Research Foundation of Korea under Contract No. R32-2008-000-10155-0.

[1] D. M. Asner *et al.*, Int. J. Mod. Phys. A **24**, 499 (2009).
[2] L. Kopke and N. Wermes, Phys. Rept. **174**, 67 (1989).
[3] H. Kowalski and T. F. Walsh, Phys. Rev. D **14**, 852 (1976).
[4] I. Peruzzi *et al.* (MARK I Collaboration), Phys. Rev. D **17**, 2901 (1978).
[5] S. Dulat, J. J. Wu and B. S. Zou, Phys. Rev. D **83**, 094032 (2011).
[6] E. Kaxiras, E. J. Moniz and M. Soyeur, Phys. Rev. D **32**, 695 (1985).
[7] J. W. Darewych, M. Horbatsch and R. Koniuk, Phys. Rev. D **28**, 1125 (1983).
[8] M. Warns, W. Pfeil and H. Rollnik, Phys. Lett. B **258**, 431 (1991).
[9] Y. Umino and F. Myhrer, Nucl. Phys. A **529**, 713 (1991); Nucl. Phys. A **554**, 593 (1993).
[10] R. Bijker, F. Iachello and A. Leviatan, Annals Phys. **284**, 89 (2000).
[11] L. Yu, X. L. Chen, W. Z. Deng and S. L. Zhu, Phys. Rev. **D** 73, 114001 (2006).
[12] T. S. Mast *et al.*, Phys. Rev. Lett. **21**, 1715 (1968).
[13] R. Bertini, Nucl. Phys. B **279**, 49 (1987); R. Bertini *et*

TABLE V: Constraint fit results for the amplitude parameterizations in terms of a singlet A, symmetric and antisymmetric charge-breaking (D, F), mass-breaking (D', F') terms and a relative phase δ as listed in Table IV. The fit is constrained to the measured branching fractions from PDG [23] and Ref. [32], as listed in Table IV, as well as the measurement in this analysis. The χ^2/d.o.f is 1.01/2.0 for the fit. Similar fitting results from Ref. [31] are also shown for comparison.

	A	D	F	D'	F'	δ
our fit	1.000 ± 0.044	-0.058 ± 0.005	0.231 ± 0.140	0.015 ± 0.028	-0.027 ± 0.045	$(76 \pm 11)^\circ$
Ref. [31]	1.000 ± 0.028	0 (fixed)	0.341 ± 0.085	0.032 ± 0.041	-0.050 ± 0.070	$(106 \pm 8)^\circ$

al., SACLAY-DPh-N-2372 (unpublished).

[14] Y. M. Antipov *et al.* (SPHINX Collaboration), Phys. Lett. B **604**, 22 (2004).

[15] S. Taylor *et al.* (CLAS Collaboration), Phys. Rev. C **71**, 054609 (2005).

[16] C. H. Wu *et al.* (Belle Collaboration), Phys. Rev. Lett. **97**, 162003 (2006).

[17] M. Ablikim *et al.* (BES Collaboration), Phys. Rev. D **83**, 012003 (2011).

[18] M. Ablikim *et al.* (BES Collaboration), Nucl. Instrum. Meth. A **614** 345, (2010).

[19] S. Agostinelli *et al.* (GEANT4 Collaboration), Nucl. Instrum. Methods Phys. Res., Sect. A **506**, 250 (2003).

[20] J. Allison *et al.*, IEEE Trans. Nucl. Sci. **53**, 270 (2006).

[21] D. J. Lange *et al.*, Nucl. Instrum. Meth. A **462**, 1 (2001).

[22] S. Jadach, B. F. L. Ward and Z. Was, Comput. Phys. Commun. **130**, 260 (2000); S. Jadach, B. F. L. Ward and Z. Was Phys. Rev. D **63**, 113009 (2001).

[23] The Review of Particle Physics, C. Amsler *et al.*, J. Phys. G **37**, 075021 (2010).

[24] J. C. Chen, G. S. Huang, X. R. Qi, D. H. Zhang, and Y. S. Zhu, Phys. Rev. D **62**, 034003 (2000).

[25] M. Ablikim *et al.* (BES Collaboration), Phys. Rev. Lett. **108**, 112003 (2012).

[26] V. V. Anashin *et al.* (KEDR Collaboration), arXiv:1012.1694 [hep-ex]

[27] R. E. Mitchell *et al.* (CLEO Collaboration), Phys. Rev. Lett. **102**, 011801 (2009).

[28] M. Ablikim *et al.* (BES Collaboration), Phys. Rev. Lett. **108**, 222002 (2012).

[29] J. G. Korner, M. Kuroda, Phys. Rev. D **16**, 2165 (1977).

[30] We also considered possible interference effects between η_c signal and non-resonance backgrounds. With the assumption of all the non-resonant backgrounds are from 0^{-+} phase space, we obtained two solutions: $\phi = 4.74 \pm 0.29$(stat.) rad (constructive) or $\phi = 1.46 \pm 0.23$(stat.) rad (destructive), where ϕ is the relative phase between η_c resonance and non-resonance amplitudes. The constructive (destructive) interference results in $\mathcal{B}(J/\psi \to \gamma\eta_c \to \gamma\Lambda\bar{\Lambda}) = (1.36 \pm 0.31(\text{stat.})) \times 10^{-5}$ ($(3.48 \pm 0.70(\text{stat.})) \times 10^{-5}$). The fit method is similar to that described in Ref. [28].

[31] D. H. Wei, J. Phys. G **36**, 115006 (2009).

[32] M. Ablikim *et al.* (BES Collaboration), arXiv:1205.1036 [hep-ex].